

# A nonlocal strain gradient refined plate model for thermal vibration analysis of embedded graphene sheets via DQM

Farzad Ebrahimi\* and Mohammad Reza Barati

Mechanical Engineering Department, Faculty of Engineering, Imam Khomeini International University, Qazvin, P.O.B. 3414916818, Iran

(Received January 5, 2018, Revised March 16, 2018, Accepted March 19, 2018)

**Abstract.** This paper develops a nonlocal strain gradient plate model for vibration analysis of graphene sheets under thermal environments. For more accurate analysis of graphene sheets, the proposed theory contains two scale parameters related to the nonlocal and strain gradient effects. Graphene sheet is modeled via a two-variable shear deformation plate theory needless of shear correction factors. Governing equations of a nonlocal strain gradient graphene sheet on elastic substrate are derived via Hamilton's principle. Differential quadrature method (DQM) is implemented to solve the governing equations for different boundary conditions. Effects of different factors such as temperature rise, nonlocal parameter, length scale parameter, elastic foundation and aspect ratio on vibration characteristics a graphene sheets are studied. It is seen that vibration frequencies and critical buckling temperatures become larger and smaller with increase of strain gradient and nonlocal parameter, respectively.

**Keywords:** thermal vibration; refined plate theory; graphene sheets; nonlocal strain gradient theory

## 1. Introduction

Graphene is an actually two-dimensional atomic crystal with exceptional electronic and mechanical properties. Many carbon based nanostructures including carbon nanotubes, nanoplates and nanobeams are considered as deformed graphene sheets (Ebrahimi and Salari 2015). In fact, analysis of graphene sheets is a basic matter in the study of the nanomaterials and nanostructures. Analysis of scale-free plates has been performed widely in the literature employing classical theories. But, such theories are not able to examine the scale effects on the nanostructures with small size. Therefore, the nonlocal elasticity theory of Eringen (Eringen 1983, Eringen and Edelen 1972) is developed taking into account small scale effects. Contrary to the local theory in which the stress state at any given point depends only on the strain state at that point, in the nonlocal theory, the stress state at a given point depends on the strain states at all points. The nonlocal elasticity theory has been broadly applied to investigate the mechanical behavior of nanoscale structures (Ebrahimi and Barati 2016a, b, c, d, e, f).

Pradhan and Murmu (2009) examined nonlocal influences on buckling behavior of a single-layer graphene sheets subjected to uniform in-plane loadings. Also, Pradhan and Kumar (2009) performed vibration study of orthotropic graphene sheets incorporating nonlocal effects using a semi-analytical approach. Application of Levy type method in stability and vibrational investigation of nanosize plates including nonlocal effects is examined by Aksencer and Aydogdu (2011). Mohammadi *et al.* (2014) performed shear buckling analysis of an orthotropic graphene sheet on elastic

substrate including thermal loading effect. In another work, Mohammadi *et al.* (2013) examined the effect of in-plane loading on nonlocal vibrational behavior of circular graphene sheets.

Also, Ansari *et al.* (2011) explored vibration response of embedded nonlocal multi-layered graphene sheets accounting for various boundary conditions. Shen *et al.* (2012) studied vibration behavior of nanomechanical mass sensor based on nonlocal graphene sheet model. They showed that vibration response of graphene sheet is significantly influenced by the mass of attached nanoparticle. Farajpour *et al.* (2012) examined static stability of nonlocal plates subjected to non-uniform in-plane edge loads. Also, Ansari and Sahmani (2013) employed molecular dynamics simulations to examine biaxial buckling behavior of single-layered graphene sheets based on nonlocal elasticity theory. They matched the results obtained by molecular dynamics simulations with those of nonlocal plate model to extract the appropriate values of nonlocal parameter. Static bending and vibrational behavior of single-layered graphene sheets on Winkler-Pasternak foundation based on a two-variable higher order shear deformation theory is studied by Sobhy (2014). Also, Narendar and Gopalakrishnan (2012) carried out size-dependent stability analysis of orthotropic nanoscale plates according to a nonlocal two-variable refined plate theory. They stated that the two variable refined plate model considers the transverse shear influences through the thickness of the plate, hence it is unnecessary to apply shear correction factors. Murmu *et al.* (2013) explored the influence of unidirectional magnetic fields on vibrational behavior of nonlocal single-layer graphene sheets resting on elastic substrate. Bessaim *et al.* (2015) presented a nonlocal quasi-3D trigonometric plate model for free vibration behavior of micro/nanoscale plates. Hashemi *et al.* (2015) studied free vibrational behavior of double viscoelastic

\*Corresponding author, Professor  
E-mail: febrahimi@eng.ikiu.ac.ir

graphene sheets coupled by visco-Pasternak medium. Ebrahimi and Shafiei (2016) examined the influence of initial shear stress on the vibration behavior of single-layered graphene sheets embedded in an elastic medium based on Reddy's higher-order shear deformation plate theory. Jiang *et al.* (2016) conducted vibration analysis of a single-layered graphene sheet-based mass sensor using the Galerkin strip distributed transfer function method. Arani *et al.* (2016) examined nonlocal vibration of axially moving graphene sheet resting on orthotropic visco-Pasternak foundation under longitudinal magnetic field. Sobhy (2016) analyzed Hygro-thermal vibrational behavior of coupled graphene sheets by an elastic medium using the two-variable plate theory. Also, Zenkour (2016) performed transient thermal analysis of graphene sheets on viscoelastic foundation based on nonlocal elasticity theory.

It is clear that all of previous papers on graphene sheets applied only the nonlocal elasticity theory to capture small scale effects. However, nonlocal elasticity theory has some limitations in accurate prediction of mechanical behavior of nanostructures. Because, nonlocal elasticity theory is unable to examine the stiffness increment observed in experimental works and strain gradient elasticity (Lam *et al.* 2003). Recently, Lim *et al.* (2015) proposed the nonlocal strain gradient theory to introduce both of the length scales into a single theory. The nonlocal strain gradient theory captures the true influence of the two length scale parameters on the physical and mechanical behavior of small size structures (Li and Hu 2016, Li *et al.* 2016, Karami *et al.* 2018). Recently, Ebrahimi and Barati (2016g, h, 2017 a, b) applied the nonlocal strain gradient theory in analysis of nanobeams. They mentioned that mechanical characteristics of nanostructures are significantly affected by stiffness-softening and stiffness-hardening mechanisms due to the nonlocal and strain gradient effects, respectively. Most recently, Ebrahimi *et al.* (2016) extended the nonlocal strain gradient theory for analysis of nanoplates to obtain the wave frequencies for a range of two scale parameters. Most recently, Li *et al.* (2018) examined the thickness effect on mechanical behaviors of NSGT nanobeams.

Based on newly developed nonlocal strain gradient theory, free vibration behavior of single-layer graphene sheets in thermal environment resting on elastic medium is examined using a refined two-variable plate theory. The theory introduces two scale parameters corresponding to nonlocal and strain gradient effects to capture both stiffness-softening and stiffness-hardening influences. Hamilton's principle is employed to obtain the governing equation of a nonlocal strain gradient graphene sheet. These equations are solved via Differential quadrature method (DQM) to obtain the natural frequencies. It is shown that vibration behavior of graphene sheets is significantly influenced by nonlocal parameter, length scale parameter, temperature rise, elastic foundation and aspect ratio.

## 2. Governing equations

The higher-order refined plate theory has the following displacement field as

$$u_1(x, y, z) = u(x, y) - z \frac{\partial w_b}{\partial x} - f(z) \frac{\partial w_s}{\partial x} \quad (1)$$

$$u_2(x, y, z) = v(x, y) - z \frac{\partial w_b}{\partial y} - f(z) \frac{\partial w_s}{\partial y} \quad (2)$$

$$u_3(x, y, z) = w_b(x, y) + w_s(x, y) \quad (3)$$

where the present theory has a trigonometric function in the following form (Ebrahimi and Barati 2016)

$$f(z) = z - \frac{h}{\pi} \sin\left(\frac{\pi z}{h}\right) \quad (4)$$

Also,  $u$  and  $v$  are displacements components of the mid-surface and  $w_b$  and  $w_s$  denote the bending and shear transverse displacement, respectively. Nonzero strains of present plate model are expressed as follows

$$\begin{Bmatrix} \varepsilon_x \\ \varepsilon_y \\ \gamma_{xy} \end{Bmatrix} = +z \begin{Bmatrix} \kappa_x^b \\ \kappa_y^b \\ \kappa_{xy}^b \end{Bmatrix} + f(z) \begin{Bmatrix} \kappa_x^s \\ \kappa_y^s \\ \kappa_{xy}^s \end{Bmatrix}, \begin{Bmatrix} \gamma_{yz} \\ \gamma_{xz} \end{Bmatrix} = g(z) \begin{Bmatrix} \gamma_{yz}^s \\ \gamma_{xz}^s \end{Bmatrix} \quad (5)$$

where  $g(z) = 1 - df/dz$  and

$$\begin{Bmatrix} \kappa_x^b \\ \kappa_y^b \\ \kappa_{xy}^b \end{Bmatrix} = \begin{Bmatrix} \frac{\partial^2 w_b}{\partial x^2} \\ \frac{\partial^2 w_b}{\partial y^2} \\ -2 \frac{\partial^2 w_b}{\partial x \partial y} \end{Bmatrix}, \begin{Bmatrix} \kappa_x^s \\ \kappa_y^s \\ \kappa_{xy}^s \end{Bmatrix} = \begin{Bmatrix} \frac{\partial^2 w_s}{\partial x^2} \\ \frac{\partial^2 w_s}{\partial y^2} \\ -2 \frac{\partial^2 w_s}{\partial x \partial y} \end{Bmatrix}, \begin{Bmatrix} \gamma_{yz}^s \\ \gamma_{xz}^s \end{Bmatrix} = \begin{Bmatrix} \frac{\partial w_s}{\partial y} \\ \frac{\partial w_s}{\partial x} \end{Bmatrix} \quad (6)$$

Also, Hamilton's principle expresses that

$$\int_0^t \delta(U - T + V) dt = 0 \quad (7)$$

in which  $U$  is strain energy,  $T$  is kinetic energy and  $V$  is work done by external loads. The variation of strain energy is calculated as

$$\delta U = \int_V \sigma_{ij} \delta \varepsilon_{ij} dV = \int_V (\sigma_x \delta \varepsilon_x + \sigma_y \delta \varepsilon_y + \sigma_{xy} \delta \gamma_{xy} + \sigma_{yz} \delta \gamma_{yz} + \sigma_{xz} \delta \gamma_{xz}) dV \quad (8)$$

Substituting Eqs. (5) and (6) into Eq. (8) yields

$$\delta U = \int_0^b \int_0^a [-M_x^b \frac{\partial^2 \delta w_b}{\partial x^2} - M_x^s \frac{\partial^2 \delta w_s}{\partial x^2} - M_y^b \frac{\partial^2 \delta w_b}{\partial y^2} - M_y^s \frac{\partial^2 \delta w_s}{\partial y^2} - 2M_{xy}^b \frac{\partial^2 \delta w_b}{\partial x \partial y} - 2M_{xy}^s \frac{\partial^2 \delta w_s}{\partial x \partial y} + Q_{yz} \frac{\partial \delta w_s}{\partial y} + Q_{xz} \frac{\partial \delta w_s}{\partial x}] dx dy \quad (9)$$

in which

$$\begin{aligned} (M_i^b, M_i^s) &= \int_{-h/2}^{h/2} (z, f) \sigma_i dz, \quad i = (x, y, xy) \\ Q_i &= \int_{-h/2}^{h/2} g \sigma_i dz, \quad i = (xz, yz) \end{aligned} \quad (10)$$

The variation of the work done by applied loads can be written as

$$\begin{aligned} \delta V &= \int_0^b \int_0^a (N_x^0 \frac{\partial(w_b + w_s)}{\partial x} \frac{\partial \delta(w_b + w_s)}{\partial x} + N_y^0 \frac{\partial(w_b + w_s)}{\partial y} \frac{\partial \delta(w_b + w_s)}{\partial y} \\ &\quad + 2\delta N_{xy}^0 \frac{\partial(w_b + w_s)}{\partial x} \frac{\partial \delta(w_b + w_s)}{\partial y} - k_w \delta(w_b + w_s) \\ &\quad + k_p (\frac{\partial(w_b + w_s)}{\partial x} \frac{\partial \delta(w_b + w_s)}{\partial x} + \frac{\partial(w_b + w_s)}{\partial y} \frac{\partial \delta(w_b + w_s)}{\partial y})) dx dy \end{aligned} \quad (11)$$

where  $N_x^0, N_y^0, N_{xy}^0$  are in-plane applied loads;  $k_w$  and  $k_p$  are Winkler and Pasternak constants.

The variation of the kinetic energy is calculated as

$$\delta K = \int_{-h/2}^{h/2} \int_{\Omega} \left[ I_0 \left( \frac{\partial(w_b + w_s)}{\partial t} \frac{\partial \delta(w_b + w_s)}{\partial t} \right) + I_1 \left( \frac{\partial w_b}{\partial x} \frac{\partial \delta w_b}{\partial x} + \frac{\partial w_b}{\partial y} \frac{\partial \delta w_b}{\partial y} \right) + K_1 \left( \frac{\partial w_b}{\partial x} \frac{\partial \delta w_b}{\partial x} + \frac{\partial w_b}{\partial y} \frac{\partial \delta w_b}{\partial y} \right) + J_2 \left( \frac{\partial^2 w_b}{\partial x^2} \frac{\partial \delta w_b}{\partial x^2} + \frac{\partial^2 w_b}{\partial y^2} \frac{\partial \delta w_b}{\partial y^2} \right) + \frac{\partial w_b}{\partial x} \frac{\partial \delta w_b}{\partial x} + \frac{\partial w_b}{\partial y} \frac{\partial \delta w_b}{\partial y} + \frac{\partial^2 w_b}{\partial x^2} \frac{\partial \delta w_b}{\partial x^2} + \frac{\partial^2 w_b}{\partial y^2} \frac{\partial \delta w_b}{\partial y^2} \right] dx dy \quad (12)$$

in which

$$(I_0, I_2, J_2, K_2) = \int_{-h/2}^{h/2} (1, z^2, zf, f^2) \rho dz \quad (13)$$

By inserting Eqs. (19)-(22) into Eq. (17) and setting the coefficients of  $\delta u, \delta v, \delta w_b$  and  $\delta w_s$  to zero, the following Euler-Lagrange equations can be obtained.

$$\frac{\partial^2 M_x^b}{\partial x^2} + 2 \frac{\partial^2 M_{xy}^b}{\partial x \partial y} + \frac{\partial^2 M_y^b}{\partial y^2} - (N^T) \nabla^2 (w_b + w_s) + k_p \left[ \frac{\partial^2 (w_b + w_s)}{\partial x^2} + \frac{\partial^2 (w_b + w_s)}{\partial y^2} \right] - k_w (w_b + w_s) = I_0 \frac{\partial^2 (w_b + w_s)}{\partial t^2} - I_2 \nabla^2 \left( \frac{\partial^2 w_b}{\partial t^2} \right) - J_2 \nabla^2 \left( \frac{\partial^2 w_s}{\partial t^2} \right) \quad (14)$$

$$\frac{\partial^2 M_x^s}{\partial x^2} + 2 \frac{\partial^2 M_{xy}^s}{\partial x \partial y} + \frac{\partial^2 M_y^s}{\partial y^2} + \frac{\partial Q_x}{\partial x} + \frac{\partial Q_y}{\partial y} - (N^T) \nabla^2 (w_b + w_s) + k_{pi} \left[ \frac{\partial^2 (w_b + w_s)}{\partial x^2} + \frac{\partial^2 (w_b + w_s)}{\partial y^2} \right] - k_w (w_b + w_s) = I_0 \frac{\partial^2 (w_b + w_s)}{\partial t^2} - J_2 \nabla^2 \left( \frac{\partial^2 w_b}{\partial t^2} \right) - K_2 \nabla^2 \left( \frac{\partial^2 w_s}{\partial t^2} \right) \quad (15)$$

where  $N_x^0 = N_y^0 = N^T, N_{xy}^0 = 0$  and thermal resultant can be expressed as

$$N^T = \int_{-h/2}^{h/2} \frac{E}{1-\nu} \alpha \Delta T dz \quad (16)$$

### 2.1 Nonlocal strain gradient nanoplate model

The newly developed nonlocal strain gradient theory (Ebrahimi *et al.* 2016) takes into account both nonlocal stress field and the strain gradient effects by introducing two scale parameters. This theory defines the stress field as

$$\sigma_{ij} = \sigma_{ij}^{(0)} - \frac{d\sigma_{ij}^{(1)}}{dx} \quad (17)$$

in which the stresses  $\sigma_{xx}^{(0)}$  and  $\sigma_{xx}^{(1)}$  are corresponding to strain  $\epsilon_{xx}$  and strain gradient  $\epsilon_{xx,x}$ , respectively as

$$\sigma_{ij}^{(0)} = \int_0^L C_{ijkl} \alpha_0(x, x', e_0 a) \epsilon'_{kl}(x') dx' \quad (18)$$

$$\sigma_{ij}^{(1)} = l^2 \int_0^L C_{ijkl} \alpha_1(x, x', e_1 a) \epsilon'_{kl,x}(x') dx' \quad (19)$$

in which  $C_{ijkl}$  are the elastic coefficients and  $e_0 a$  and  $e_1 a$  capture the nonlocal effects and  $l$  captures the strain gradient effects. When the nonlocal functions  $\alpha_0(x, x', e_0 a)$  and  $\alpha_1(x, x', e_1 a)$  satisfy the developed conditions by Eringen (Eringen 1983), the constitutive relation of nonlocal strain gradient theory has the following form

$$[1 - (e_0 a)^2 \nabla^2][1 - (e_1 a)^2 \nabla^2] \sigma_{ij} = C_{ijkl} [1 - (e_0 a)^2 \nabla^2] \epsilon_{kl} - C_{ijkl} l^2 [1 - (e_0 a)^2 \nabla^2] \nabla^2 \epsilon_{kl} \quad (20)$$

in which  $\nabla^2$  denotes the Laplacian operator. Considering  $e_1 = e_0 = e$ , the general constitutive relation in Eq. (22a) becomes

$$[1 - (ea)^2 \nabla^2] \sigma_{ij} = C_{ijkl} [1 - l^2 \nabla^2] \epsilon_{kl} \quad (21)$$

To consider thermal effects Eq. (21) can be written as (Ebrahimi *et al.* 2016)

$$[1 - (ea)^2 \nabla^2] \sigma_{ij} = C_{ijkl} [1 - l^2 \nabla^2] (\epsilon_{kl} - \alpha_{ij} T) \quad (22)$$

where  $\alpha_{ij}$  is thermal expansion coefficient. Finally, the constitutive relations of nonlocal strain gradient theory can be expressed by

$$(1 - \mu \nabla^2) \begin{Bmatrix} \sigma_x \\ \sigma_y \\ \sigma_{xy} \\ \sigma_{yz} \\ \sigma_{xz} \end{Bmatrix} = (1 - \lambda \nabla^2) \begin{pmatrix} Q_{11} & Q_{12} & 0 & 0 & 0 \\ Q_{12} & Q_{22} & 0 & 0 & 0 \\ 0 & 0 & Q_{66} & 0 & 0 \\ 0 & 0 & 0 & Q_{44} & 0 \\ 0 & 0 & 0 & 0 & Q_{55} \end{pmatrix} \begin{Bmatrix} \epsilon_x - \alpha \Delta T \\ \epsilon_y - \alpha \Delta T \\ \gamma_{xy} \\ \gamma_{yz} \\ \gamma_{xz} \end{Bmatrix} \quad (23)$$

where

$$Q_{11} = Q_{22} = \frac{E}{1-\nu^2}, Q_{12} = \nu Q_{11}, Q_{44} = Q_{55} = Q_{66} = \frac{E}{2(1+\nu)} \quad (24)$$

where  $\mu = (e_0 a)^2$  and  $\lambda = l^2$ . Inserting Eq. (10) in Eq. (23) gives

$$(1 - \mu \nabla^2) \begin{Bmatrix} M_x^b \\ M_y^b \\ M_{xy}^b \end{Bmatrix} = (1 - \lambda \nabla^2) \begin{pmatrix} D_{11} & D_{12} & 0 \\ D_{12} & D_{22} & 0 \\ 0 & 0 & D_{66} \end{pmatrix} \begin{Bmatrix} \frac{\partial^2 w_b}{\partial x^2} \\ \frac{\partial^2 w_b}{\partial y^2} \\ -2 \frac{\partial^2 w_b}{\partial x \partial y} \end{Bmatrix} + \begin{pmatrix} D_{11}^s & D_{12}^s & 0 \\ D_{12}^s & D_{22}^s & 0 \\ 0 & 0 & D_{66}^s \end{pmatrix} \begin{Bmatrix} \frac{\partial^2 w_s}{\partial x^2} \\ \frac{\partial^2 w_s}{\partial y^2} \\ -2 \frac{\partial^2 w_s}{\partial x \partial y} \end{Bmatrix} \quad (25)$$

$$(1 - \mu \nabla^2) \begin{Bmatrix} M_x^s \\ M_y^s \\ M_{xy}^s \end{Bmatrix} = (1 - \lambda \nabla^2) \begin{pmatrix} D_{11}^s & D_{12}^s & 0 \\ D_{12}^s & D_{22}^s & 0 \\ 0 & 0 & D_{66}^s \end{pmatrix} \begin{Bmatrix} \frac{\partial^2 w_b}{\partial x^2} \\ \frac{\partial^2 w_b}{\partial y^2} \\ -2 \frac{\partial^2 w_b}{\partial x \partial y} \end{Bmatrix} + \begin{pmatrix} H_{11}^s & H_{12}^s & 0 \\ H_{12}^s & H_{22}^s & 0 \\ 0 & 0 & H_{66}^s \end{pmatrix} \begin{Bmatrix} \frac{\partial^2 w_s}{\partial x^2} \\ \frac{\partial^2 w_s}{\partial y^2} \\ -2 \frac{\partial^2 w_s}{\partial x \partial y} \end{Bmatrix} \quad (26)$$

$$(1 - \mu \nabla^2) \begin{Bmatrix} Q_x \\ Q_y \end{Bmatrix} = (1 - \lambda \nabla^2) \begin{pmatrix} A_{44}^s & 0 \\ 0 & A_{55}^s \end{pmatrix} \begin{Bmatrix} \frac{\partial w_s}{\partial x} \\ \frac{\partial w_s}{\partial y} \end{Bmatrix} \quad (27)$$

in which the cross-sectional rigidities are defined as follows

$$\begin{Bmatrix} D_{11}, D_{11}^s, H_{11}^s \\ D_{12}, D_{12}^s, H_{12}^s \\ D_{66}, D_{66}^s, H_{66}^s \end{Bmatrix} = \int_{-h/2}^{h/2} Q_{11} (z^2, zf, f^2) \begin{Bmatrix} 1 \\ \nu \\ \frac{1-\nu}{2} \end{Bmatrix} dz \quad (28)$$

$$A_{44}^s = A_{55}^s = \int_{-h/2}^{h/2} g^2 \frac{E}{2(1+\nu)} dz \quad (29)$$

The governing equations of nonlocal strain gradient graphene sheet in terms of the displacement are obtained by inserting Eqs. (25)-(27), into Eqs. (14)-(15) as follows

$$\begin{aligned} & -D_{11} \left[ \frac{\partial^4 w_b}{\partial x^4} - \lambda \left( \frac{\partial^6 w_b}{\partial x^6} + \frac{\partial^6 w_b}{\partial x^4 \partial y^2} \right) \right] - 2(D_{12} + 2D_{66}) \frac{\partial^4 w_b}{\partial x^2 \partial y^2} - \lambda \left( \frac{\partial^6 w_b}{\partial x^4 \partial y^2} + \frac{\partial^6 w_b}{\partial x^2 \partial y^4} \right) \\ & - D_{22} \left[ \frac{\partial^4 w_b}{\partial y^4} - \lambda \left( \frac{\partial^6 w_b}{\partial y^6} + \frac{\partial^6 w_b}{\partial y^2 \partial x^2} \right) \right] - D_{11}^s \left[ \frac{\partial^4 w_s}{\partial x^4} - \lambda \left( \frac{\partial^6 w_s}{\partial x^6} + \frac{\partial^6 w_s}{\partial x^4 \partial y^2} \right) \right] \\ & - 2(D_{12}^s + 2D_{66}^s) \left[ \frac{\partial^4 w_s}{\partial x^2 \partial y^2} - \lambda \left( \frac{\partial^6 w_s}{\partial x^4 \partial y^2} + \frac{\partial^6 w_s}{\partial x^2 \partial y^4} \right) \right] - D_{22}^s \left[ \frac{\partial^4 w_s}{\partial y^4} - \lambda \left( \frac{\partial^6 w_s}{\partial y^6} + \frac{\partial^6 w_s}{\partial y^2 \partial x^2} \right) \right] \\ & - I_{01} \left[ \frac{\partial^2 (w_b + w_s)}{\partial t^2} - \mu \left( \frac{\partial^4 (w_b + w_s)}{\partial t^2 \partial x^2} + \frac{\partial^4 (w_b + w_s)}{\partial t^2 \partial y^2} \right) \right] + I_2 \left[ \frac{\partial^4 w_b}{\partial x^2 \partial t^2} + \frac{\partial^4 w_b}{\partial y^2 \partial t^2} - \mu \left( \frac{\partial^6 w_b}{\partial t^2 \partial x^4} \right. \right. \\ & \left. \left. + 2 \frac{\partial^6 w_b}{\partial t^2 \partial x^2 \partial y^2} + \frac{\partial^6 w_b}{\partial t^2 \partial y^4} \right) \right] + J_2 \left[ \frac{\partial^4 w_s}{\partial x^2 \partial t^2} + \frac{\partial^4 w_s}{\partial y^2 \partial t^2} - \mu \left( \frac{\partial^6 w_s}{\partial t^2 \partial x^4} + 2 \frac{\partial^6 w_s}{\partial t^2 \partial x^2 \partial y^2} + \frac{\partial^6 w_s}{\partial t^2 \partial y^4} \right) \right] \\ & - (N^T - k_p) \left[ \frac{\partial^2 (w_b + w_s)}{\partial x^2} + \frac{\partial^2 (w_b + w_s)}{\partial y^2} - \mu \left( \frac{\partial^4 (w_b + w_s)}{\partial x^4} + 2 \frac{\partial^4 (w_b + w_s)}{\partial x^2 \partial y^2} + \frac{\partial^4 (w_b + w_s)}{\partial y^4} \right) \right] \\ & - k_w [(w_b + w_s) + \mu \left( \frac{\partial^2 (w_b + w_s)}{\partial x^2} + \frac{\partial^2 (w_b + w_s)}{\partial y^2} \right)] = 0 \end{aligned} \quad (30)$$

$$\begin{aligned}
 & -D_{11}^4 \left[ \frac{\partial^4 w_b}{\partial x^4} - \lambda \left( \frac{\partial^6 w_b}{\partial x^6} + \frac{\partial^6 w_b}{\partial x^4 \partial y^2} \right) \right] + A_{33} \left[ \frac{\partial^2 w_s}{\partial x^2} - \lambda \left( \frac{\partial^4 w_s}{\partial x^4} + \frac{\partial^4 w_s}{\partial x^2 \partial y^2} \right) \right] \\
 & + A_{44} \left[ \frac{\partial^2 w_s}{\partial y^2} - \lambda \left( \frac{\partial^4 w_s}{\partial y^4} + \frac{\partial^4 w_s}{\partial y^2 \partial x^2} \right) \right] - 2(D_{12} + 2D_{66}) \left[ \frac{\partial^4 w_b}{\partial x^2 \partial y^2} - \lambda \left( \frac{\partial^6 w_b}{\partial x^4 \partial y^2} + \frac{\partial^6 w_b}{\partial x^2 \partial y^4} \right) \right] \\
 & - D_{22}^4 \left[ \frac{\partial^4 w_b}{\partial y^4} - \lambda \left( \frac{\partial^6 w_b}{\partial y^6} + \frac{\partial^6 w_b}{\partial y^4 \partial x^2} \right) \right] - H_{11}^4 \left[ \frac{\partial^4 w_s}{\partial x^4} - \lambda \left( \frac{\partial^6 w_s}{\partial x^6} + \frac{\partial^6 w_s}{\partial x^4 \partial y^2} \right) \right] \\
 & - 2(H_{12} + 2H_{66}) \left[ \frac{\partial^4 w_s}{\partial x^2 \partial y^2} - \lambda \left( \frac{\partial^6 w_s}{\partial x^4 \partial y^2} + \frac{\partial^6 w_s}{\partial x^2 \partial y^4} \right) \right] - H_{22}^4 \left[ \frac{\partial^4 w_s}{\partial y^4} - \lambda \left( \frac{\partial^6 w_s}{\partial y^6} + \frac{\partial^6 w_s}{\partial y^4 \partial x^2} \right) \right] \\
 & - I_0 \left[ \frac{\partial^2 (w_b + w_s)}{\partial t^2} - \mu \left( \frac{\partial^4 (w_b + w_s)}{\partial t^2 \partial x^2} + \frac{\partial^4 (w_b + w_s)}{\partial t^2 \partial y^2} \right) \right] + J_x \left[ \frac{\partial^4 w_b}{\partial x^2 \partial t^2} + \frac{\partial^4 w_s}{\partial y^2 \partial t^2} - \mu \left( \frac{\partial^6 w_b}{\partial t^2 \partial x^4} \right. \right. \\
 & \left. \left. + 2 \frac{\partial^6 w_b}{\partial t^2 \partial x^2 \partial y^2} + \frac{\partial^6 w_b}{\partial t^2 \partial y^4} \right) \right] + K_x \left[ \frac{\partial^4 w_s}{\partial x^2 \partial t^2} + \frac{\partial^4 w_s}{\partial y^2 \partial t^2} - \mu \left( \frac{\partial^6 w_s}{\partial t^2 \partial x^4} + 2 \frac{\partial^6 w_s}{\partial t^2 \partial x^2 \partial y^2} + \frac{\partial^6 w_s}{\partial t^2 \partial y^4} \right) \right] \\
 & - (N^T - k_p) \left[ \frac{\partial^2 (w_b + w_s)}{\partial x^2} + \frac{\partial^2 (w_b + w_s)}{\partial y^2} \right] - \mu \left[ \frac{\partial^4 (w_b + w_s)}{\partial x^4} + 2 \frac{\partial^4 (w_b + w_s)}{\partial x^2 \partial y^2} \right. \\
 & \left. + \frac{\partial^4 (w_b + w_s)}{\partial y^4} \right] - k_w [(w_b + w_s) + \mu \left( \frac{\partial^2 (w_b + w_s)}{\partial x^2} + \frac{\partial^2 (w_b + w_s)}{\partial y^2} \right)] = 0
 \end{aligned} \tag{31}$$

### 3. Solution by DQM

In this section, differential quadrature method (DQM) is implemented to solve the governing equations of nonlocal strain gradient graphene sheets. In DQM, derivative of a function  $F$  at a given grid point  $(x_i, y_j)$  is considered as weighted linear sum of all functional values within the computational domain as

$$\frac{d^n F}{dx^n} \Big|_{x=x_i} = \sum_{j=1}^N c_{ij}^{(n)} F(x_j) \tag{32}$$

where

$$C_{ij}^{(1)} = \frac{\pi(x_i)}{(x_i - x_j) \pi(x_j)} \quad i, j = 1, 2, \dots, N, \quad i \neq j \tag{33}$$

in which  $\pi(x_i)$  is defined by

$$\pi(x_i) = \prod_{j=1, j \neq i}^N (x_i - x_j) \tag{34}$$

And when  $i = j$

$$C_{ij}^{(1)} = c_{ii}^{(1)} = - \sum_{k=1, k \neq i}^N C_{ik}^{(1)}, \quad i = 1, 2, \dots, N, \quad i \neq k, \tag{35}$$

Also, weighting coefficients of higher order derivatives are defined as

$$\begin{aligned}
 C_{ij}^{(2)} &= \sum_{k=1}^N C_{ik}^{(1)} C_{kj}^{(1)} \\
 C_{ij}^{(3)} &= \sum_{k=1}^N C_{ik}^{(1)} C_{kj}^{(2)} = \sum_{k=1}^N C_{ik}^{(2)} C_{kj}^{(1)} \\
 C_{ij}^{(4)} &= \sum_{k=1}^N C_{ik}^{(1)} C_{kj}^{(3)} = \sum_{k=1}^N C_{ik}^{(3)} C_{kj}^{(1)} \quad i, j \\
 &= 1, 2, \dots, N. \\
 C_{ij}^{(5)} &= \sum_{k=1}^N C_{ik}^{(1)} C_{kj}^{(4)} = \sum_{k=1}^N C_{ik}^{(4)} C_{kj}^{(1)} \\
 C_{ij}^{(6)} &= \sum_{k=1}^N C_{ik}^{(1)} C_{kj}^{(5)} = \sum_{k=1}^N C_{ik}^{(5)} C_{kj}^{(1)}
 \end{aligned} \tag{36}$$

Table 1 Comparison of natural frequency of a graphene sheet for various nonlocal and foundation parameters (a/h=10)

$\mu$	$K_w=0, K_p=0$		$K_w=100, K_p=0$		$K_w=0, K_p=20$	
	Sobhy (2014)	present	Sobhy (2014)	present	Sobhy (2014)	present
0	1.93861	1.93861	2.18396	2.18396	2.7841	2.78410
1	1.17816	1.17816	1.54903	1.54903	2.31969	2.31969
2	0.92261	0.92261	1.36479	1.36479	2.20092	2.20092
3	0.78347	0.78347	1.27485	1.27485	2.14629	2.14629
4	0.69279	0.69279	1.22122	1.22122	2.11486	2.11486

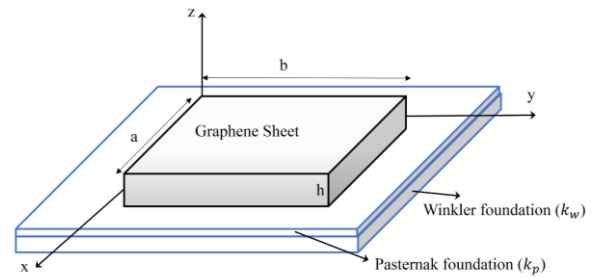


Fig. 1 Configuration of graphene sheet resting on elastic substrate

In the present method, the distribution of grid points according to Gauss-Chebyshev-Lobatto model is defined by

$$\begin{aligned}
 x_i &= \frac{a}{2} \left[ 1 - \cos \left( \frac{i-1}{N-1} \pi \right) \right] \quad i = 1, 2, \dots, N, \\
 y_j &= \frac{b}{2} \left[ 1 - \cos \left( \frac{j-1}{M-1} \pi \right) \right] \quad j = 1, 2, \dots, M,
 \end{aligned} \tag{37}$$

Also, the time derivatives of displacement field can be calculated as

$$w_b(x, y, t) = W_b(x, y) e^{i\omega t} \tag{38}$$

$$w_s(x, y, t) = W_s(x, y) e^{i\omega t} \tag{39}$$

in which  $W_b$  and  $W_n$  are unknown coefficients and  $\omega$  is the eigenfrequency. Boundary conditions based on present plate model are

$$w_b = w_s = 0, \quad \frac{\partial^2 w_b}{\partial x^2} = \frac{\partial^2 w_s}{\partial x^2} = \frac{\partial^2 w_b}{\partial y^2} = \frac{\partial^2 w_s}{\partial y^2} = 0 \quad \text{simply-supported edge} \tag{40}$$

$$w_b = w_s = 0, \quad \frac{\partial w_b}{\partial x} = \frac{\partial w_s}{\partial x} = \frac{\partial w_b}{\partial y} = \frac{\partial w_s}{\partial y} = 0 \quad \text{clamped edge} \tag{41}$$

By modifying weighting coefficients, it is possible to consider mentioned boundary conditions. For fully simply-supported edges, we have

$$\begin{aligned}
 \bar{C}_{1,j}^{(2)} &= \bar{C}_{N,j}^{(2)} = 0, \quad i = 1, 2, \dots, M, \\
 \bar{C}_{i,1}^{(2)} &= \bar{C}_{i,M}^{(2)} = 0, \quad i = 1, 2, \dots, N.
 \end{aligned} \tag{42}$$

Other weighting coefficients can be written as

$$\begin{aligned}
 \bar{C}_{ij}^{(3)} &= \sum_{k=1}^N C_{ik}^{(1)} \bar{C}_{kj}^{(2)} \\
 \bar{C}_{ij}^{(4)} &= \sum_{k=1}^N C_{ik}^{(1)} \bar{C}_{kj}^{(3)}
 \end{aligned} \tag{43}$$

Substituting Eq. (36) into the governing Eqs. (30) and (31), we have

$$\begin{aligned}
 & -D_{11} \left[ \sum_{k=1}^M \bar{C}_{1k}^{(4)} W_{b,k,j} - \lambda \left( \sum_{k=1}^M \bar{C}_{1k}^{(6)} W_{b,k,j} + \sum_{k=1}^M \sum_{l=1}^M \bar{C}_{1k}^{(4)} \bar{A}_{jk}^{(2)} W_{b,k,l} \right) \right] \\
 & -2(D_{12} + 2D_{60}) \left[ \sum_{k=1}^M \bar{C}_{1k}^{(2)} \bar{A}_{jk}^{(2)} W_{b,k,l} - \lambda \left( \sum_{k=1}^M \bar{C}_{1k}^{(4)} \bar{A}_{jk}^{(2)} W_{b,k,l} \right. \right. \\
 & \left. \left. + \sum_{k=1}^M \sum_{l=1}^M \bar{C}_{1k}^{(2)} \bar{A}_{jl}^{(4)} W_{b,k,l} \right) \right] - D_{21} \left[ \sum_{k=1}^M \bar{A}_{jk}^{(2)} W_{b,k,l} - \lambda \left( \sum_{k=1}^M \bar{A}_{jk}^{(6)} W_{b,k,l} \right. \right. \\
 & \left. \left. + \sum_{k=1}^M \sum_{l=1}^M \bar{C}_{1k}^{(2)} \bar{A}_{jk}^{(4)} W_{b,k,l} \right) \right] - D_{11} \left[ \sum_{k=1}^M \bar{C}_{1k}^{(2)} W_{b,k,j} - \lambda \left( \sum_{k=1}^M \bar{C}_{1k}^{(6)} W_{b,k,j} \right. \right. \\
 & \left. \left. + \sum_{k=1}^M \sum_{l=1}^M \bar{C}_{1k}^{(2)} \bar{A}_{jk}^{(4)} W_{b,k,l} \right) \right] - 2(D_{12} + 2D_{60}) \left[ \sum_{k=1}^M \sum_{l=1}^M \bar{C}_{1k}^{(2)} \bar{A}_{jk}^{(2)} W_{b,k,l} \right. \\
 & \left. - \lambda \left( \sum_{k=1}^M \sum_{l=1}^M \bar{C}_{1k}^{(4)} \bar{A}_{jk}^{(2)} W_{b,k,l} + \sum_{k=1}^M \sum_{l=1}^M \bar{C}_{1k}^{(2)} \bar{A}_{jl}^{(4)} W_{b,k,l} \right) \right] - D_{21} \left[ \sum_{k=1}^M \bar{A}_{jk}^{(2)} W_{b,k,l} \right. \\
 & \left. - \lambda \left( \sum_{k=1}^M \bar{A}_{jk}^{(6)} W_{b,k,l} + \sum_{k=1}^M \sum_{l=1}^M \bar{C}_{1k}^{(2)} \bar{A}_{jk}^{(4)} W_{b,k,l} \right) \right] + \omega^2 J_0 \left[ \sum_{k=1}^M \bar{C}_{1k}^{(0)} (W_b + W_s)_{k,j} \right. \\
 & \left. - \mu \left( \sum_{k=1}^M \bar{C}_{1k}^{(2)} (W_b + W_s)_{k,j} + \sum_{k=1}^M \bar{A}_{jk}^{(2)} (W_b + W_s)_{k,l} \right) \right] - \omega^2 J_1 \left[ \sum_{k=1}^M \bar{C}_{1k}^{(2)} W_{b,k,j} \right. \\
 & \left. + \sum_{k=1}^M \bar{A}_{jk}^{(2)} W_{s,k} - \mu \left( \sum_{k=1}^M \bar{C}_{1k}^{(4)} W_{b,k,j} + 2 \sum_{k=1}^M \sum_{l=1}^M \bar{C}_{1k}^{(2)} \bar{A}_{jk}^{(2)} W_{b,k,l} \right) \right. \\
 & \left. - \omega^2 J_1 \left[ \sum_{k=1}^M \bar{C}_{1k}^{(2)} W_{s,k,j} + \sum_{k=1}^M \bar{A}_{jk}^{(2)} W_{s,k,l} - \mu \left( \sum_{k=1}^M \bar{C}_{1k}^{(4)} W_{s,k,j} + 2 \sum_{k=1}^M \sum_{l=1}^M \bar{C}_{1k}^{(2)} \bar{A}_{jk}^{(2)} W_{s,k,l} \right) \right. \right. \\
 & \left. \left. + \sum_{k=1}^M \bar{A}_{jk}^{(2)} W_{s,k} \right) \right] - (N^T - k_p) \left[ \sum_{k=1}^M \bar{C}_{1k}^{(2)} (W_b + W_s)_{k,j} + \sum_{k=1}^M \bar{A}_{jk}^{(2)} (W_b + W_s)_{k,l} \right. \\
 & \left. - \mu \left( \sum_{k=1}^M \bar{C}_{1k}^{(4)} (W_b + W_s)_{k,j} + 2 \sum_{k=1}^M \sum_{l=1}^M \bar{C}_{1k}^{(2)} \bar{A}_{jk}^{(2)} (W_b + W_s)_{k,l} + \sum_{k=1}^M \bar{A}_{jk}^{(2)} (W_b + W_s)_{k,l} \right) \right] \\
 & - k_s \left[ \sum_{k=1}^M \bar{C}_{1k}^{(0)} (W_b + W_s)_{k,j} - \mu \left( \sum_{k=1}^M \bar{C}_{1k}^{(2)} (W_b + W_s)_{k,j} + \sum_{k=1}^M \bar{A}_{jk}^{(2)} (W_b + W_s)_{k,l} \right) \right] = 0
 \end{aligned} \quad (44)$$

$$\begin{aligned}
 & -D_{11} \left[ \sum_{k=1}^M \bar{C}_{1k}^{(4)} W_{b,k,j} - \lambda \left( \sum_{k=1}^M \bar{C}_{1k}^{(6)} W_{b,k,j} + \sum_{k=1}^M \sum_{l=1}^M \bar{C}_{1k}^{(4)} \bar{A}_{jk}^{(2)} W_{b,k,l} \right) \right] - 2(D_{12} + 2D_{60}) \left[ \sum_{k=1}^M \sum_{l=1}^M \bar{C}_{1k}^{(2)} \bar{A}_{jk}^{(2)} W_{b,k,l} \right. \\
 & \left. - \lambda \left( \sum_{k=1}^M \sum_{l=1}^M \bar{C}_{1k}^{(4)} \bar{A}_{jk}^{(2)} W_{b,k,l} + \sum_{k=1}^M \sum_{l=1}^M \bar{C}_{1k}^{(2)} \bar{A}_{jl}^{(4)} W_{b,k,l} \right) \right] + A_{63} \left[ \sum_{k=1}^M \bar{C}_{1k}^{(2)} W_{s,k,j} - \lambda \left( \sum_{k=1}^M \bar{C}_{1k}^{(6)} W_{s,k,j} \right. \right. \\
 & \left. \left. + \sum_{k=1}^M \sum_{l=1}^M \bar{C}_{1k}^{(2)} \bar{A}_{jk}^{(4)} W_{s,k,l} \right) \right] - A_{61} \left[ \sum_{k=1}^M \bar{A}_{jk}^{(2)} W_{s,k} - \lambda \left( \sum_{k=1}^M \bar{A}_{jk}^{(6)} W_{s,k} + \sum_{k=1}^M \sum_{l=1}^M \bar{C}_{1k}^{(2)} \bar{A}_{jk}^{(4)} W_{s,k,l} \right) \right] \\
 & - D_{21} \left[ \sum_{k=1}^M \bar{A}_{jk}^{(2)} W_{b,k,l} - \lambda \left( \sum_{k=1}^M \bar{A}_{jk}^{(6)} W_{b,k,l} + \sum_{k=1}^M \sum_{l=1}^M \bar{C}_{1k}^{(2)} \bar{A}_{jk}^{(4)} W_{b,k,l} \right) \right] - H_{11} \left[ \sum_{k=1}^M \bar{C}_{1k}^{(2)} W_{s,k,j} - \lambda \left( \sum_{k=1}^M \bar{C}_{1k}^{(6)} W_{s,k,j} \right. \right. \\
 & \left. \left. + \sum_{k=1}^M \sum_{l=1}^M \bar{C}_{1k}^{(2)} \bar{A}_{jk}^{(4)} W_{s,k,l} \right) \right] - 2(H_{12} + 2H_{60}) \left[ \sum_{k=1}^M \sum_{l=1}^M \bar{C}_{1k}^{(2)} \bar{A}_{jk}^{(2)} W_{s,k,l} - \lambda \left( \sum_{k=1}^M \sum_{l=1}^M \bar{C}_{1k}^{(4)} \bar{A}_{jk}^{(2)} W_{s,k,l} \right. \right. \\
 & \left. \left. + \sum_{k=1}^M \sum_{l=1}^M \bar{C}_{1k}^{(2)} \bar{A}_{jl}^{(4)} W_{s,k,l} \right) \right] - H_{21} \left[ \sum_{k=1}^M \bar{A}_{jk}^{(2)} W_{s,k} - \lambda \left( \sum_{k=1}^M \bar{A}_{jk}^{(6)} W_{s,k} + \sum_{k=1}^M \sum_{l=1}^M \bar{C}_{1k}^{(2)} \bar{A}_{jk}^{(4)} W_{s,k,l} \right) \right] \\
 & + \omega^2 J_1 \left[ \sum_{k=1}^M \bar{C}_{1k}^{(2)} (W_b + W_s)_{k,j} - \mu \left( \sum_{k=1}^M \bar{C}_{1k}^{(4)} (W_b + W_s)_{k,j} + \sum_{k=1}^M \bar{A}_{jk}^{(2)} (W_b + W_s)_{k,l} \right) \right] - \omega^2 J_2 \left[ \sum_{k=1}^M \bar{C}_{1k}^{(2)} W_{b,k,j} \right. \\
 & \left. + \sum_{k=1}^M \bar{A}_{jk}^{(2)} W_{s,k} - \mu \left( \sum_{k=1}^M \bar{C}_{1k}^{(4)} W_{b,k,j} + 2 \sum_{k=1}^M \sum_{l=1}^M \bar{C}_{1k}^{(2)} \bar{A}_{jk}^{(2)} W_{b,k,l} + \sum_{k=1}^M \bar{A}_{jk}^{(2)} W_{s,k} \right) \right] - \omega^2 K_{21} \left[ \sum_{k=1}^M \bar{C}_{1k}^{(2)} W_{s,k,j} \right. \\
 & \left. + \sum_{k=1}^M \bar{A}_{jk}^{(2)} W_{s,k} - \mu \left( \sum_{k=1}^M \bar{C}_{1k}^{(4)} W_{s,k,j} + 2 \sum_{k=1}^M \sum_{l=1}^M \bar{C}_{1k}^{(2)} \bar{A}_{jk}^{(2)} W_{s,k,l} + \sum_{k=1}^M \bar{A}_{jk}^{(2)} W_{s,k} \right) \right] - (N^T - k_p) \left[ \sum_{k=1}^M \bar{C}_{1k}^{(2)} (W_b + W_s)_{k,j} \right. \\
 & \left. + \sum_{k=1}^M \bar{A}_{jk}^{(2)} (W_b + W_s)_{k,l} - \mu \left( \sum_{k=1}^M \bar{C}_{1k}^{(4)} (W_b + W_s)_{k,j} + 2 \sum_{k=1}^M \sum_{l=1}^M \bar{C}_{1k}^{(2)} \bar{A}_{jk}^{(2)} (W_b + W_s)_{k,l} + \sum_{k=1}^M \bar{A}_{jk}^{(2)} (W_b + W_s)_{k,l} \right) \right] \\
 & - k_s \left[ \sum_{k=1}^M \bar{C}_{1k}^{(0)} (W_b + W_s)_{k,j} - \mu \left( \sum_{k=1}^M \bar{C}_{1k}^{(2)} (W_b + W_s)_{k,j} + \sum_{k=1}^M \bar{A}_{jk}^{(2)} (W_b + W_s)_{k,l} \right) \right] = 0
 \end{aligned} \quad (45)$$

Where  $\bar{C}$  and  $\bar{A}$  denote the weighting coefficients in  $x$  and  $y$  directions, respectively. Setting the coefficient matrix of above equations leads to the following eigenvalue problem

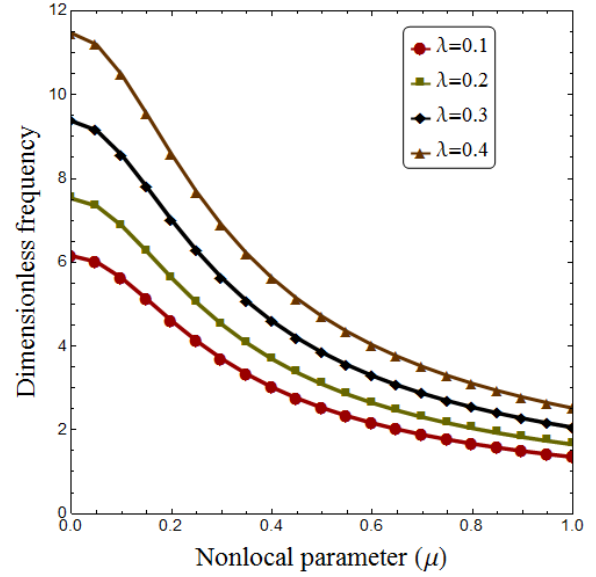
$$([K] + \omega^2 [M]) \begin{Bmatrix} W_b \\ W_s \end{Bmatrix} = 0 \quad (46)$$

where  $[M]$  and  $[K]$  are the mass matrix and stiffness matrix, respectively. Finally, setting the coefficient matrix to zero gives the natural frequencies. It should be noted that calculations are performed based on the following dimensionless quantities

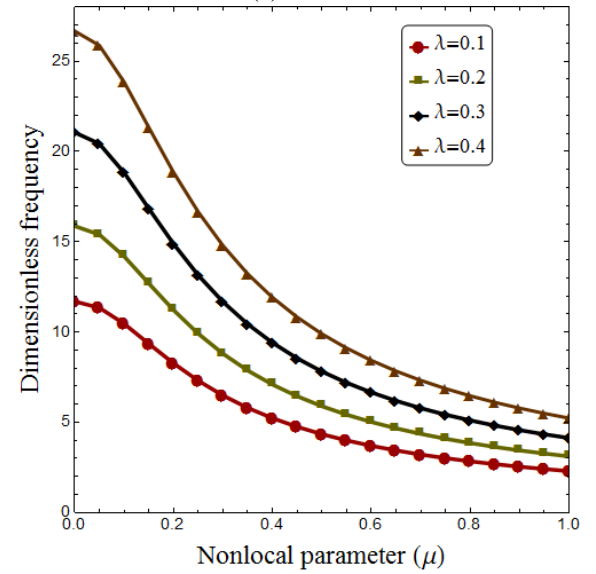
$$\hat{\omega} = \omega \frac{a^2}{h} \sqrt{\frac{\rho}{E}}, \quad K_w = k_w \frac{a^4}{D}, \quad K_p = k_p \frac{a^2}{D}, \quad D^* = \frac{Eh^3}{12(1-\nu^2)}, \quad \mu = \frac{ea}{a}, \quad \lambda = \frac{l}{a} \quad (47)$$

#### 4. Numerical results and discussions

This section is devoted to study the hygro-thermo-mechanical vibration behavior of nonlocal strain gradient graphene sheets on elastic substrate based on a two-variable shear deformation theory. The model introduces two scale coefficients related to nonlocal and strain gradient effects for more accurate analysis of graphene sheets. Material properties of the graphene sheet are:  $E=1$  TPa,  $\nu=0.19$ ,  $\alpha=1.6 \times 10^{-6}$  1/K and  $\rho=2300$  kg/m<sup>3</sup>. Also, thickness of graphene sheet is considered as  $h=0.34$  nm. Natural



(a) SSSS

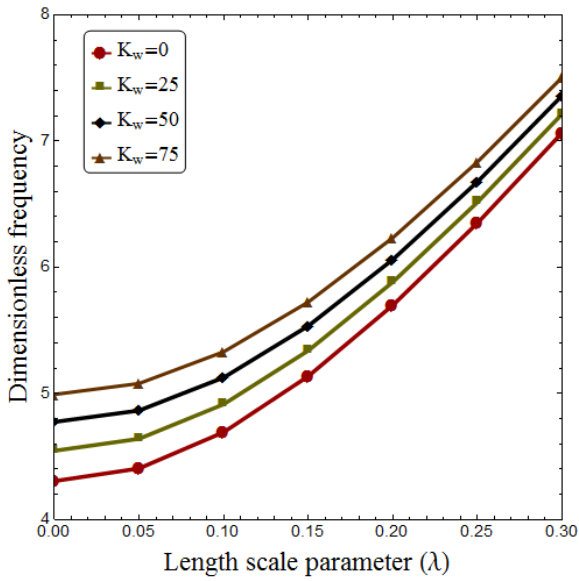


(b) CCCC

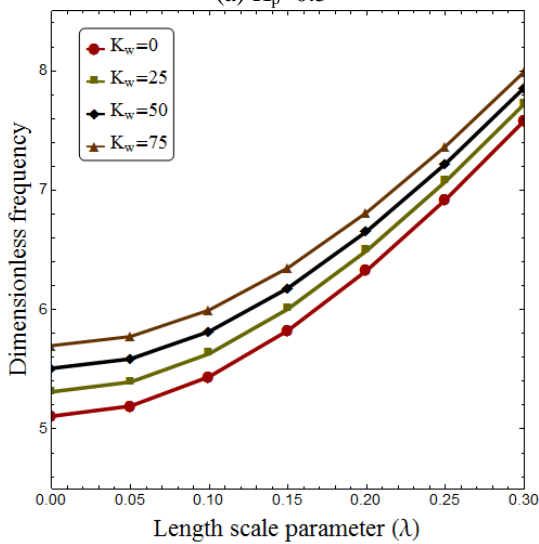
Fig. 2 Variation of dimensionless frequency versus nonlocal parameter for different strain gradient parameters ( $a/h=10$ ,  $\Delta T=0$ )

frequencies of a graphene sheet are validated with those obtained by Sobhy (2014) for various nonlocal parameters ( $\mu=0, 1, 2, 3, 4$  nm<sup>2</sup>) and foundation constants ( $\{K_w, K_p\}=\{(0,0), (100,0), (0,20)\}$ ). Obtained frequencies via present DQ method are in excellent agreement with those of exact solution presented by Sobhy (2014), as tabulated in Table 1. For comparison study, the strain gradient parameter is set to zero ( $\lambda=0$ ).

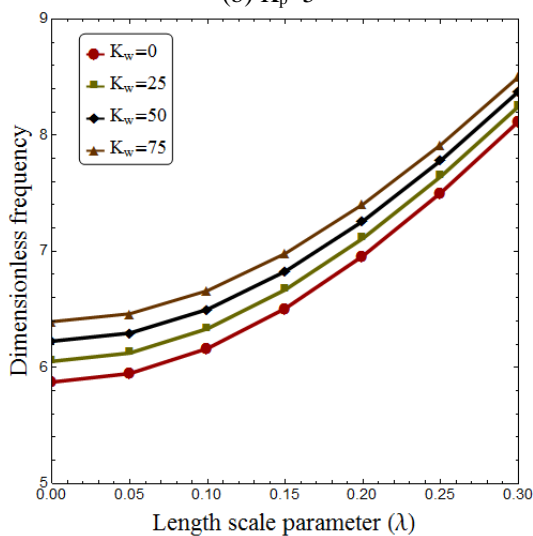
Examination of nonlocal and strain gradient effects on vibration frequencies of graphene sheets for SSSS and CCCC boundary conditions is presented in Fig. 2 when  $a/h=10$ . In this figure, various values of nonlocal parameter ( $\mu=0 \sim 1$ ) and length scale parameter ( $\lambda=0.1, 0.2, 0.3, 0.4$ ) are considered. When  $\mu=0$  and  $\lambda=0$ , the results based on classical continuum mechanics are rendered. It is observed that natural frequency of graphene sheet reduces with



(a)  $K_p=0.5$

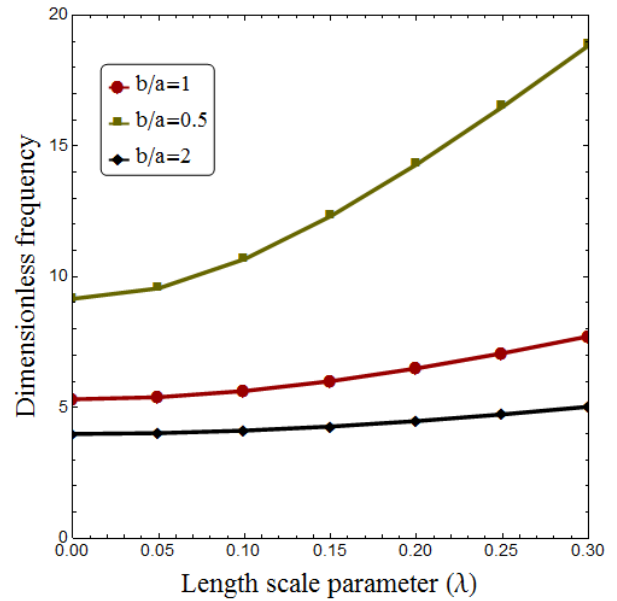


(b)  $K_p=5$

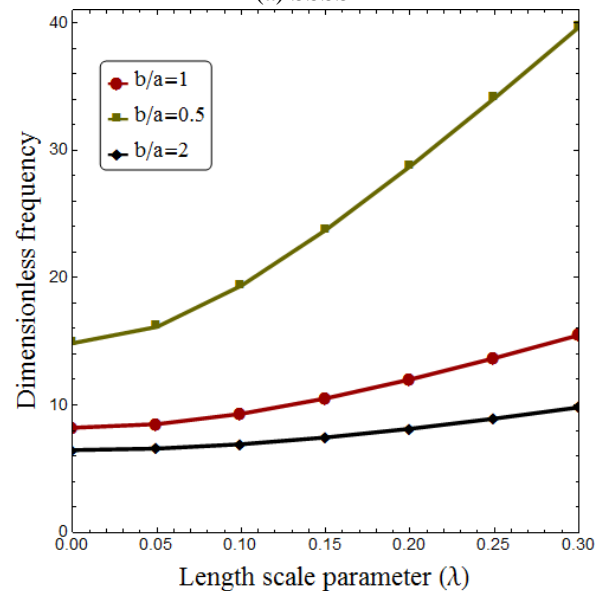


(c)  $K_p=10$

Fig. 3 Variation of dimensionless frequency versus length scale parameter for different Winkler and Pasternak constants ( $a/h=10, \Delta T=0, \mu=0.2$ )



(a) SSSS

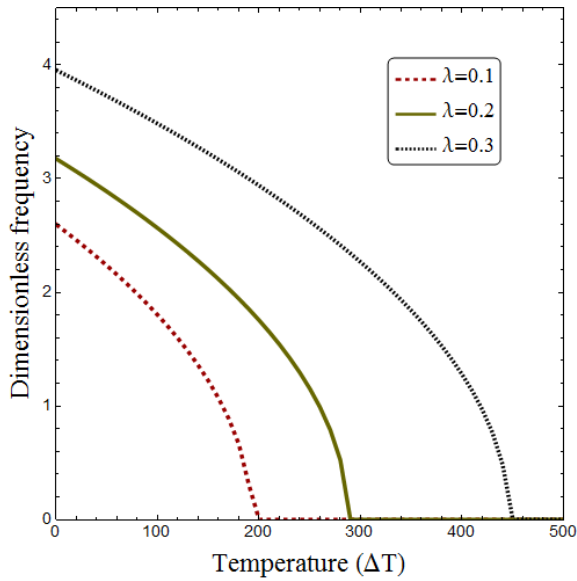


(b) CCCC

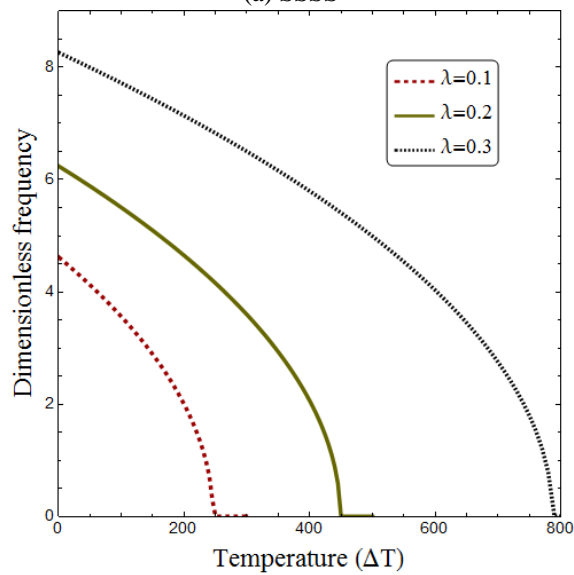
Fig. 4 Variation of dimensionless frequency versus length scale parameter for different aspect ratios ( $a/h=10, \Delta T=0, K_p=5, K_w=25, \mu=0.2$ )

increase of nonlocal parameter for every kind of boundary condition. This observation indicates that nonlocal parameter exerts a stiffness-softening effect which leads to lower vibration frequencies. But, effect of nonlocal parameter on the magnitude of natural frequencies depends on the value of strain gradient or length scale parameter. In fact, natural frequency of graphene sheet increases with increase of length scale parameter which highlights the stiffness-hardening effect due to the strain gradients. Also, it is clear that making the graphene sheet more rigid by imposing clamped edges leads to higher natural frequencies.

Fig. 3 demonstrates the variation of dimensionless frequency versus length scale parameter for different



(a) SSSS



(b) CCCC

Fig. 5 Variation of dimensionless frequency versus temperature change for different strain gradient parameters ( $a/h=30, K_p=K_w=0, \mu=0.5$ )

Winkler and Pasternak constants when  $a/h=10, \Delta T=0$  and  $\mu=0.2$ . However, it is clear that natural frequency of graphene sheet depends on the values of both Winkler and Pasternak parameters. In fact, Pasternak layer provides a continuous interaction with graphene sheet, while Winkler layer has a discontinuous interaction with the graphene sheet. Increasing Winkler and Pasternak parameters leads to larger frequencies by enhancing the bending rigidity of graphene sheets. But, Pasternak layer shows more increasing effect on natural frequencies compared with Winkler layer. It is found that magnitude of natural frequency for various values of foundation parameters depends on the strain gradient effect. As previously mentioned, increasing of length scale parameter leads to larger natural frequencies for every values of foundation parameters.

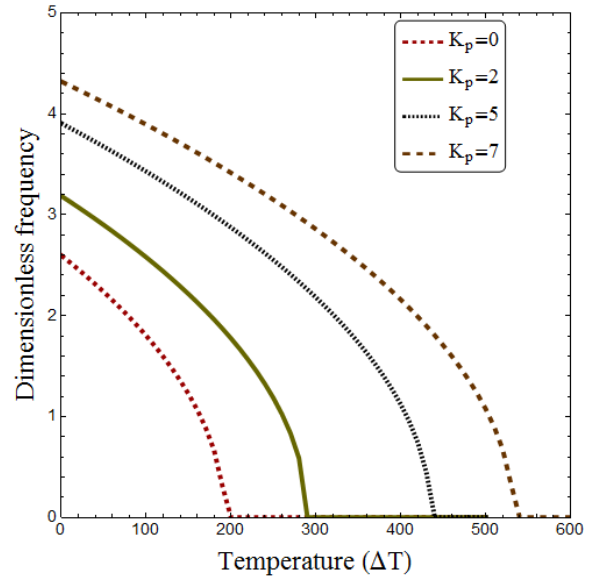
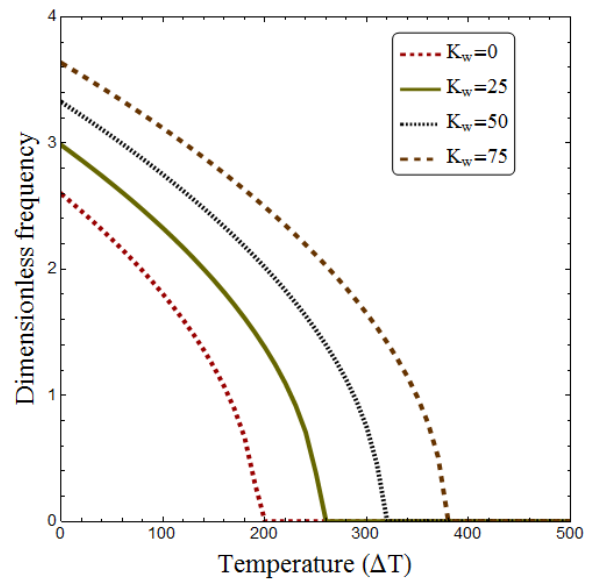


Fig. 6 Variation of dimensionless frequency versus temperature change for different foundation parameters ( $a/h=30, \mu=0.5, \lambda=0.1$ )

Effect of plate aspect ratio ( $b/a$ ) on natural frequencies of graphene sheets with respect to length scale parameter is plotted in Fig. 4 at  $a/h=10, \Delta T=0, K_p=5, K_w=25$  and  $\mu=0.2$ . It is found that increasing aspect ratio reduces the vibration frequencies of graphene sheets. This is due to the more flexibility of grapheme sheets with higher aspect ratios. However, effect of length scale parameter on vibration frequencies depend on the value of aspect ratio. In fact, graphene sheets with lower aspect ratios are more affected by length scale parameter. Therefore, strain gradient effect which is neglected in all previous studies on graphene sheets should be incorporated into nonlocal elasticity theory to obtain more reasonable results.

Fig. 5 shows the variation of dimensionless frequency of graphene sheets with respect to temperature rise ( $\Delta T$ ) for different length scale parameters when  $a/h=30$ . It should be pointed out that increase of temperature degrades the plate stiffness and natural frequencies reduce until a critical point

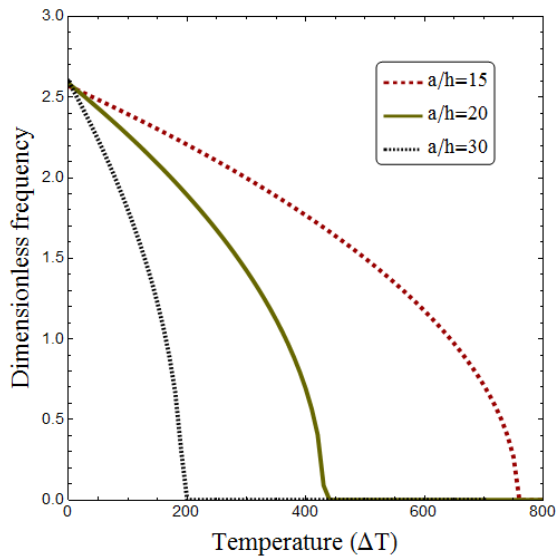


Fig. 7 Variation of dimensionless frequency versus temperature change for different side-to-thickness ratios ( $\mu=0.5$ ,  $\lambda=0.1$ )

in which the frequencies become zero. At this point, the graphene sheet buckles and does not oscillate. However, obtained critical buckling temperatures depend on the value of length scale parameter. In fact, inclusion of length scale parameter in nonlocal strain gradient theory leads to higher critical temperatures compared with nonlocal theory. So, it can be concluded that critical temperatures obtained by nonlocal elasticity theory are underestimated. As a consequence, it is very important to consider both nonlocal and length scale parameters in analysis of graphene sheets.

Effect of Winkler and Pasternak layers of elastic foundation on natural frequencies and critical buckling temperatures of nonlocal strain gradient graphene sheets is depicted in Fig. 6 at  $a/h=30$ ,  $\mu=0.5$  and  $\lambda=0.1$ . It is observed that values of critical temperatures are affected by the Winkler and Pasternak constants. In fact, increase of Winkler and Pasternak constants makes the plate more rigid and the critical temperature shifts to the right. In other words, increasing the magnitude of elastic foundation parameters leads to postponement in thermal buckling of graphene sheets.

Fig. 7 depicts the variation of dimensionless frequency versus temperature change for different side-to-thickness ratios ( $a/h$ ) at  $\mu=0.5$ ,  $\lambda=0.1$ . It is seen that graphene sheets with higher side-to-thickness ratios are more flexible and they have lower vibration frequencies. Accordingly, graphene sheets with higher side-to-thickness ratios have smaller critical buckling temperatures. It is also found that effect of side-to-thickness ratio on natural frequencies is not sensible at lower temperature differences. In other words, as the temperature rises, effect of side-to-thickness ratio on natural frequencies becomes more important.

## 5. Conclusions

In this paper, nonlocal strain gradient theory is employed to investigate free vibration behavior of single-layer graphene

sheets in thermal environment resting on elastic medium using a refined two-variable plate theory. The theory introduces two scale parameters corresponding to nonlocal and strain gradient effects to capture both stiffness-softening and stiffness-hardening influences. Hamilton's principle is employed to obtain the governing equation of a nonlocal strain gradient graphene sheet. These equations are solved via DQ method to obtain the natural frequencies. It is observed that natural frequency of graphene sheet reduces with increase of nonlocal parameter. In contrast, natural frequency increases with increase of length scale parameter which highlights the stiffness-hardening effect due to the strain gradients. Also, increase of temperature degrades the plate stiffness and natural frequencies reduce until a critical point in which the frequencies become zero. It is seen that nonlocal strain gradient theory provides larger critical temperatures than nonlocal elasticity theory. In fact, considering strain gradient effects leads to postponement in thermal buckling of graphene sheets. All these observations are affected by the Winkler-Pasternak medium which enhances the plate stiffness and increases the natural frequencies.

## References

- Aksencer, T. and Aydogdu, M. (2011), "Levy type solution method for vibration and buckling of nanoplates using nonlocal elasticity theory", *Phys. E: Low-Dimens. Syst. Nanostruct.*, **43**(4), 954-959.
- Ansari, R. and Sahmani, S. (2013), "Prediction of biaxial buckling behavior of single-layered graphene sheets based on nonlocal plate models and molecular dynamics simulations", *Appl. Math. Model.*, **37**(12), 7338-7351.
- Ansari, R., Arash, B. and Rouhi, H. (2011), "Vibration characteristics of embedded multi-layered graphene sheets with different boundary conditions via nonlocal elasticity", *Compos. Struct.*, **93**(9), 2419-2429.
- Arani, A.G., Haghparast, E. and Zarei, H.B. (2016), "Nonlocal vibration of axially moving graphene sheet resting on orthotropic visco-Pasternak foundation under longitudinal magnetic field", *Phys. B: Condens. Matt.*, **495**, 35-49.
- Ebrahimi, F. and Barati, M.R. (2016), "A nonlocal higher-order refined magneto-electro-viscoelastic beam model for dynamic analysis of smart nanostructures", *Int. J. Eng. Sci.*, **107**, 183-196.
- Ebrahimi, F. and Barati, M.R. (2016), "A unified formulation for dynamic analysis of nonlocal heterogeneous nanobeams in hygro-thermal environment", *Appl. Phys. A*, **122**(9), 792.
- Ebrahimi, F. and Barati, M.R. (2016), "Hygrothermal buckling analysis of magnetically actuated embedded higher order functionally graded nanoscale beams considering the neutral surface position", *J. Therm. Stress.*, **39**(10), 1210-1229.
- Ebrahimi, F. and Barati, M.R. (2016), "Size-dependent dynamic modeling of inhomogeneous curved nanobeams embedded in elastic medium based on nonlocal strain gradient theory", *J. Mecha. Eng. Sci.*, 0954406216668912.
- Ebrahimi, F. and Barati, M.R. (2016), "Static stability analysis of smart magneto-electro-elastic heterogeneous nanoplates embedded in an elastic medium based on a four-variable refined plate theory", *Smart Mater. Struct.*, **25**(10), 105014.
- Ebrahimi, F. and Barati, M.R. (2016), "Vibration analysis of nonlocal beams made of functionally graded material in thermal environment", *Eur. Phys. J. Plus*, **131**(8), 279.

- Ebrahimi, F. and Barati, M.R. (2016), "Vibration analysis of smart piezoelectrically actuated nanobeams subjected to magneto-electrical field in thermal environment", *J. Vibr. Contr.*, 1077546316646239.
- Ebrahimi, F. and Barati, M.R. (2016), "Wave propagation analysis of quasi-3D FG nanobeams in thermal environment based on nonlocal strain gradient theory", *Appl. Phys. A*, **122**(9), 843.
- Ebrahimi, F. and Barati, M.R. (2017), "A nonlocal strain gradient refined beam model for buckling analysis of size-dependent shear-deformable curved FG nanobeams", *Compos. Struct.*, **159**, 174-182.
- Ebrahimi, F. and Barati, M.R. (2017), "Hygrothermal effects on vibration characteristics of viscoelastic FG nanobeams based on nonlocal strain gradient theory", *Compos. Struct.*, **159**, 433-444.
- Ebrahimi, F. and Salari, E. (2015), "Thermo-mechanical vibration analysis of a single-walled carbon nanotube embedded in an elastic medium based on higher-order shear deformation beam theory", *J. Mech. Sci. Technol.*, **29**(9), 3797-3803.
- Ebrahimi, F. and Shafiei, N. (2016), "Influence of initial shear stress on the vibration behavior of single-layered graphene sheets embedded in an elastic medium based on Reddy's higher-order shear deformation plate theory", *Mech. Adv. Mater. Struct.*, 1-41.
- Ebrahimi, F., Barati, M.R. and Dabbagh, A. (2016), "A nonlocal strain gradient theory for wave propagation analysis in temperature-dependent inhomogeneous nanoplates", *Int. J. Eng. Sci.*, **107**, 169-182.
- Eringen, A.C. (1983), "On differential equations of nonlocal elasticity and solutions of screw dislocation and surface waves", *J. Appl. Phys.*, **54**(9), 4703-4710.
- Eringen, A.C. and Edelen, D.G.B. (1972), "On nonlocal elasticity", *Int. J. Eng. Sci.*, **10**(3), 233-248.
- Farajpour, A., Shahidi, A.R., Mohammadi, M. and Mahzoon, M. (2012), "Buckling of orthotropic micro/nanoscale plates under linearly varying in-plane load via nonlocal continuum mechanics", *Compos. Struct.*, **94**(5), 1605-1615.
- Hashemi, S.H., Mehrabani, H. and Ahmadi-Savadkoochi, A. (2015), "Exact solution for free vibration of coupled double viscoelastic graphene sheets by viscoPasternak medium", *Compos. Part B: Eng.*, **78**, 377-383.
- Jiang, R.W., Shen, Z.B. and Tang, G.J. (2016), "Vibration analysis of a single-layered graphene sheet-based mass sensor using the Galerkin strip distributed transfer function method", *Acta Mech.*, 1-12.
- Karami, B., Shahsavari, D. and Li, L. (2018), "Hygrothermal wave propagation in viscoelastic graphene under in-plane magnetic field based on nonlocal strain gradient theory", *Phys. E: Low-Dimens. Syst. Nanostruct.*, **97**, 317-327.
- Lam, D.C.C., Yang, F., Chong, A.C.M., Wang, J. and Tong, P. (2003), "Experiments and theory in strain gradient elasticity", *J. Mech. Phys. Sol.*, **51**(8), 1477-1508.
- Li, L., Tang, H. and Hu, Y. (2018), "The effect of thickness on the mechanics of nanobeams", *Int. J. Eng. Sci.*, **123**, 81-91.
- Lim, C.W., Zhang, G. and Reddy, J.N. (2015), "A higher-order nonlocal elasticity and strain gradient theory and its applications in wave propagation", *J. Mech. Phys. Sol.*, **78**, 298-313.
- Mohammadi, M., Farajpour, A., Moradi, A. and Ghayour, M. (2014), "Shear buckling of orthotropic rectangular graphene sheet embedded in an elastic medium in thermal environment", *Compos. Part B: Eng.*, **56**, 629-637.
- Mohammadi, M., Goodarzi, M., Ghayour, M. and Farajpour, A. (2013), "Influence of in-plane pre-load on the vibration frequency of circular graphene sheet via nonlocal continuum theory", *Compos. Part B: Eng.*, **51**, 121-129.
- Murmu, T., McCarthy, M.A. and Adhikari, S. (2013), "In-plane magnetic field affected transverse vibration of embedded single-layer graphene sheets using equivalent nonlocal elasticity approach", *Compos. Struct.*, **96**, 57-63.
- Narendar, S. and Gopalakrishnan, S. (2012), "Scale effects on buckling analysis of orthotropic nanoplates based on nonlocal two-variable refined plate theory", *Acta Mech.*, **223**(2), 395-413.
- Pradhan, S.C. and Kumar, A. (2011), "Vibration analysis of orthotropic graphene sheets using nonlocal elasticity theory and differential quadrature method", *Compos. Struct.*, **93**(2), 774-779.
- Pradhan, S.C. and Murmu, T. (2009), "Small scale effect on the buckling of single-layered graphene sheets under biaxial compression via nonlocal continuum mechanics", *Comput. Mater. Sci.*, **47**(1), 268-274.
- Shen, Z.B., Tang, H.L., Li, D.K. and Tang, G.J. (2012), "Vibration of single-layered graphene sheet-based nanomechanical sensor via nonlocal Kirchhoff plate theory", *Comput. Mater. Sci.*, **61**, 200-205.
- Sobhy, M. (2014), "Thermomechanical bending and free vibration of single-layered graphene sheets embedded in an elastic medium", *Phys. E: Low-Dimens. Syst. Nanostruct.*, **56**, 400-409.
- Sobhy, M. (2016), "Hygrothermal vibration of orthotropic double-layered graphene sheets embedded in an elastic medium using the two-variable plate theory", *Appl. Math. Model.*, **40**(1), 85-99.
- Zenkour, A.M. (2016), "Nonlocal transient thermal analysis of a single-layered graphene sheet embedded in viscoelastic medium", *Phys. E: Low-Dimens. Syst. Nanostruct.*, **79**, 87-97.

CC